FULL PAPERS

High-Density Gold Nanoparticles Supported on a $[Ru(bpy)_3]^{2+}$-Doped Silica/Fe_3O_4 Nanocomposite: Facile Preparation, Magnetically Induced Immobilization, and Applications in ECL Detection

Shaojun Guo,[a, b] Jing Li,[a, b] and Erkang Wang*[a, b]

Dedicated to Professor Ryoji Noyori on the occasion of his 70th birthday

Abstract: A large-scale process combined sonication with self-assembly techniques for the preparation of high-density gold nanoparticles supported on a $[Ru(bpy)_3]^{2+}$-doped silica/Fe_3O_4 nanocomposite (GNRSF) is provided. The obtained hybrid nanomaterials containing Fe_3O_4 spheres have high saturation magnetization, which leads to their effective immobilization on the surface of an ITO electrode through simple manipulation by an external magnetic field (without the need of a special immobilization apparatus). Furthermore, this hybrid nanomaterial film exhibits a good and very stable electro-chemiluminescence (ECL) behavior, which gives a linear response for tri-propylamine (TPA) concentrations between 5 μM and 0.21 mM, with a detection limit in the micromolar range. The sensitivity of this ECL sensor can be easily controlled by the amount of $[Ru(bpy)_3]^{2+}$ immobilized on the hybrid nanomaterials (that is, varying the amount of $[Ru(bpy)_3]^{2+}$ during GNRSF synthesis).

Keywords: electrochemiluminescence · magnetic nanoparticles · nanostructures · ruthenium · sensors

Introduction

Electrochemiluminescence (ECL) has attracted considerable attention during the past several decades due to its versatility, good temporal and spatial control, very low background signal, and straightforward optical setup. It has become an important and valuable detection method in analytical chemistry and has been used for detection in chromatography[1] and capillary electrophoresis.[2] Moreover, the applications of ECL are found widely in chemical sensing,[3] imaging,[4] lasing,[5] immunoassays, and DNA analyses.[6] Among all ECL systems, $[Ru(bpy)_3]^{2+}$ is one of the most extensively studied compounds owing to its stability, reversibility, sensitivity, and capacity to undergo ECL at room temperature in aqueous solution. To develop regenerable ECL-based sensors and detection devices and to simplify the detection system, considerable attention has been paid to the immobilization of $[Ru(bpy)_3]^{2+}$ at the electrode surface. To date, many methods for the effective immobilization of $[Ru(bpy)_3]^{2+}$ on solid electrode surfaces have been developed.[7–13] Prominent examples include the immobilization of $[Ru(bpy)_3]^{2+}$ in polymer,[7] Nafion film,[8] TiO_2–Nafion composite films,[9] carbon nanotube-based nanocomposite films,[10] sol-gels,[11] Pt nanoparticle-based nanocomposites,[12] and silica nanoparticles.[13] More recently, a solution-based self-assembly strategy has been employed to prepare novel, robust $[Ru(bpy)_3]^{2+}$-containing supramolecular microstructures for highly efficient ECL detection.[14] Although the above self-assembly methods could complete the efficient immobilization of $[Ru(bpy)_3]^{2+}$, the application in ECL sensors is not acceptable because the obtained aggregate is difficult to firmly immobilize on the electrode surface.

In contrast, magnetic nanoparticles have been the focus of intense research in a wide range of disciplines such as magnetic fluids, catalysis, biotechnology/biomedicine, magnetic resonance imaging, data storage, and environmental remediation.[15] Magnetic nanoparticle-based immobilization of $[Ru(bpy)_3]^{2+}$ is a promising approach toward the construction of very stable ECL sensors. For example, Lee and co-workers[16] reported a highly sensitive and stable $[Ru(bpy)_3]^{2+}$ ECL sensor based on the multilayer films of

[a] S. Guo, J. Li, Prof. E. Wang
State Key Laboratory of Electroanalytical Chemistry
Changchun Institute of Applied Chemistry
Chinese Academy of Sciences, Changchun, Jilin 130022 (P.R. China)
Fax: (+86) 431-85689711
E-mail: ekwang@ciac.jl.cn

[b] S. Guo, J. Li, Prof. E. Wang
Graduate School of the Chinese Academy of Sciences
Beijing, 100039 (P.R. China)

Nafion-stabilized magnetic nanoparticles formed on a platinum electrode surface. Dong and colleagues[17] successfully prepared a new type of bifunctional nanoparticle containing a magnetic core and a $[Ru(bpy)_3]^{2+}$-encapsulated luminescent shell by using the Stöber method. The resulting bifunctional nanoparticles exhibited excellent ECL performance. However, the above preparation process is complex, and the bifunctional nanoparticles obtained have low saturation magnetization, which will probably lead to their poor immobilization.

Herein we report a large-scale process that combines sonication with a self-assembly technique for the preparation of high-density gold nanoparticles supported on $[Ru(bpy)_3]^{2+}$-doped silica/Fe_3O_4 nanocomposite (GNRSF). The obtained hybrid nanomaterials containing $[Ru(bpy)_3]^{2+}$ have high saturation magnetization, which leads to effective immobilization at the surface of indium tin oxide (ITO) electrodes without the need of a special immobilization apparatus. High-density gold nanoparticles were employed as an accelerating agent for completing effective electron transfer between $[Ru(bpy)_3]^{2+}$ and the ITO electrode. Most interestingly, direct placement of GNRSF on a bare ITO electrode with simultaneous control of the obtained GNRSF film by an external magnetic field (placed at the side of the beaker), produced good and very stable ECL behavior.

Results and Discussion

The morphology of the products was investigated by scanning electron microscopy (SEM) and transmission electron microscopy (TEM). Figure 1a shows a typical SEM image of the as-prepared Fe_3O_4 spheres coated on the silicon substrate. As shown, the silicon substrate is fully covered with Fe_3O_4 spheres that have a relatively narrow size distribution. From the TEM analysis (Figure 1b), it was determined that the Fe_3O_4 spheres have an average diameter of ~350 nm. There have been several reports of the direct coating of magnetic nanoparticles with silica.[18] For magnetic oxide in particular, no primer was required to promote the deposition and adhesion of the silica shell under certain conditions,
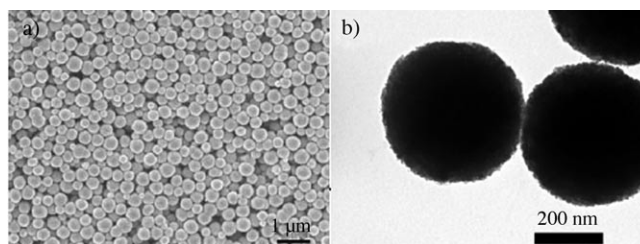

Figure 1. Representative a) SEM and b) TEM images of the Fe_3O_4 spheres prepared.

because the iron oxide surface has a strong affinity toward silica.[18]

In the work reported herein, a simple sonication approach to functionalize Fe_3O_4 with a $[Ru(bpy)_3]^{2+}$-doped silica layer is reported. Note that sonication probably provides a suitably homogeneous environment for silica growth by preventing Fe_3O_4 sedimentation. After functionalization with NH_2 groups, the above nanocomposite was mixed with gold nanoparticles to generate a high-density coverage of nanoparticles supported on the $[Ru(bpy)_3]^{2+}$-doped silica/Fe_3O_4 nanocomposite. The NH_2 groups act as a good linker for effectively adsorbing high-density gold nanoparticles on the nanocomposite surface; gold nanoparticles act as the electron-accelerating agents for enhancing the rate of electron transfer between $[Ru(bpy)_3]^{2+}$ and the ITO electrode. Typical SEM images of the obtained GNRSF at various magnifications are shown in Figure 2a–c. In Figure 2a, it can be seen that a uniform nanocomposite film was formed on the surface of the ITO electrode. The magnified image (Figure 2c) indicates that high-density gold nanoparticles were located on the surface of nanocomposite. Structural details are revealed by the TEM image (Figure 2d); the nanocomposite surface supports a great number of gold nanoparticles with a diameter of ~13 nm.

Abstract in Chinese:

基于超声和自组装技术，建立了制备高密度的金纳米粒子载体的吡啶钌掺杂的二氧化硅/Fe₃O₄ 纳米复合物的新方法。所得到的包含 Fe₃O₄ 球的杂化纳米材料具有高的磁饱和值。通过简单地施加外部磁场，该新材料可被有效地固定在 ITO 电极表面。此吡啶钌掺杂的杂化纳米膜修饰的磁控电极界面展现了优异的电化学发光性质，对三丙胺的检测线性范围为 5 μM 到 0.21 mM，检测限在 μM 级别。值一提的是，此灵敏度可以简单的通过固定在纳米复合物中吡啶钌的量来控制（在合成纳米复合物时加不同量的吡啶钌）。
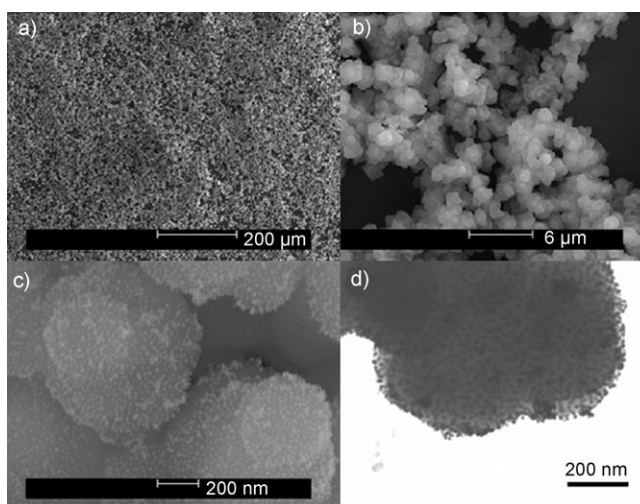
Figure 2. a–c) Representative SEM images of the as-prepared GNRSF at various magnifications (indicated); d) typical TEM image of the as-prepared GNRSF.

The chemical composition of GNRSF was determined by energy-dispersive X-ray spectroscopy (EDX, Figure 3a) and X-ray maps analysis of the product coated on the ITO sub-
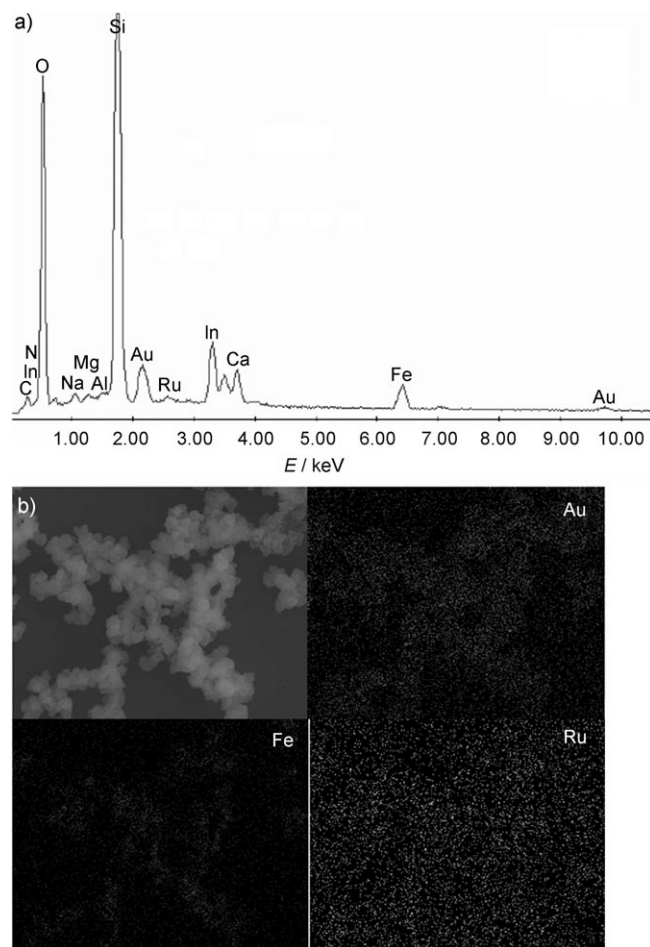

Figure 3. a) EDX spectrum and b) X-ray maps of the as-prepared GNRSF.

strate (Figure 3b). The EDX spectrum (Figure 3a) shows peaks corresponding to Au, Fe, and Ru, along with other peaks that originate from the substrate. The corresponding X-ray maps (Figure 3b) reveal that Au, Fe, and Ru have a relatively uniform distribution in the GNRSF. Based on these observations, it can be concluded that the Fe_3O_4/silica is present in the form of core/shell structures. Magnetization curves, as shown in Figure 4a, are measured on powder samples of Fe_3O_4 spheres (line A) and GNRSF (line B) at room temperature. Both exhibit negligible coercivity and remanence, and their saturation magnetization is 92.5 and 20.5 $emu\,g^{-1}$, respectively. Compared with the previous literature,[17] the relatively high saturation magnetization of GNRSF makes it quite amenable to complete magnetically induced immobilization for practical applications through simple manipulation by an external magnetic field.

To test the ECL behavior of the GNRSF prepared, we acquired the cyclic voltammogram (CV), the ECL intensity–potential curve, and the ECL intensity–time curve of the

GNRSF coated on an ITO electrode. Figure 4b shows the CV acquired at a scan rate of 100 $mV\,s^{-1}$ in 100 mM phosphate buffer (PBS, pH 7.5). A pair of redox waves appeared at ~1.1 V (versus Ag/AgCl) attributed to the one-electron redox reaction of $[Ru(bpy)_3]^{2+}$.[14] Another pair of redox waves that appeared at 0.89 and 0.48 V probably resulted from the oxidation and reduction of the gold nanoparticles.[14a] Figure 4c shows the corresponding ECL intensity–potential curves in the absence (trace A) and presence (trace B) of TPA. The onset of luminescence occurs near 0.9 V, and the ECL peak intensity occurs near 1.2 V, at which $[Ru(bpy)_3]^{2+}$ is electrochemically oxidized. Clearly, the addition of TPA gives a marked increase in the ECL intensity, indicating good sensitivity of this ECL sensor. Figure 4d shows the corresponding ECL intensity–time curves in the absence (trace A) and presence of 5 μM (trace B) and 210 μM (trace C) TPA in PBS (pH 7.5) under continuous potential scanning for 11 cycles. The relative standard deviation was <1%. In addition, the $[Ru(bpy)_3]^{2+}$ ECL sensor based on GNRSF gave a linear response for TPA concentrations between 5 μM and 0.21 mM, with a detection limit in the micromolar range. Notably, the sensitivity of the ECL sensor can be easily controlled by the amount of $[Ru(bpy)_3]^{2+}$ immobilized (that is, varying the amount of $[Ru(bpy)_3]^{2+}$ during GNRSF synthesis). Furthermore, the long-term storage stability of this sensor is good (two weeks), and the nanocomposite film does not come off when controlled by an external magnetic field; this may be attributed to the following facts: the strong electrostatic interaction between positively charged $[Ru(bpy)_3]^{2+}$ and negatively charged silica nanoparticles, and the magnetically induced immobilization caused by Fe_3O_4 spheres with high saturation magnetization. These observations suggest that the resulting $[Ru(bpy)_3]^{2+}$-containing nanocomposites exhibit good and very stable ECL behavior and therefore hold great promise for solid-state ECL detection in capillary electrophoresis (CE) or CE microchips.

Conclusions

This is the first report of a simple sonication method for the synthesis of ECL sensor materials (GNRSF) at room temperature. The electrochemical data indicate that these nanocomposites, containing $[Ru(bpy)_3]^{2+}$ and Fe_3O_4 spheres, exhibit good and very stable ECL behavior and thus provide a new type of nanocomposite material for solid-state ECL detection in capillary electrophoresis or CE microchips.
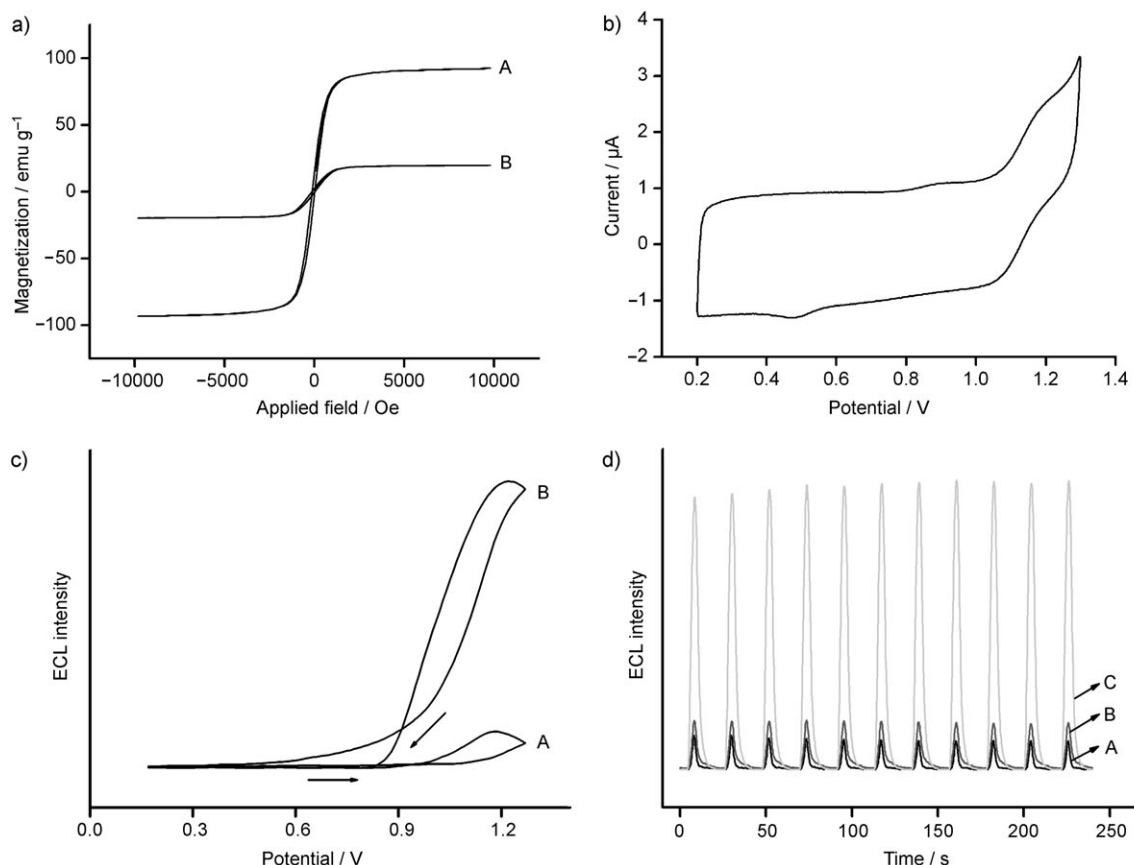
Experimental Section

Figure 4. a) Magnetization curves of Fe_3O_4 spheres (trace A) and GNRSF (trace B). b) CV of the GNRSF coated on an ITO electrode at a scan rate of $100\ mV\,s^{-1}$. c) ECL intensity–potential curves of the GNRSF coated on an ITO electrode in PBS (100 mM, pH 7.5) in the absence (trace A) and presence (trace B) of TPA (210 μM). d) ECL intensity–time curves of the GNRSF coated on an ITO electrode in PBS (100 mM, pH 7.5) in the absence (trace A) and presence of 5 μM (trace B) and 210 μM (trace C) TPA in PBS (100 mM, pH 7.5) under continuous potential scanning for 11 cycles.

Apparatus: Scanning electron microscopy (SEM) images were generated with a Philips XL-30 ESEM at an accelerating voltage of 15 kV. The samples for SEM characterization were prepared by placing 20 μL of the suspension on the ITO substrate and allowing the solvent to slowly evaporate at room temperature. TEM measurements were made on a Hitachi H-8100 EM with an accelerating voltage of 200 kV. The sample for TEM characterization was prepared by placing a drop of prepared solution on carbon-coated copper grid and drying at room temperature. Hysteresis loops were collected on a Quantum Design superconducting quantum interference device (SQUID) magnetometer (LakeShore 7307) at 296 K. Cyclic voltammetry experiments were performed on a model 800 electrochemical analyzer, and ECL signals were detected on a model MPI-A capillary electrophoresis ECL system (Xi'an Remax Electronics Inc., Xi'an, China) with the voltage of the photomultiplier tube (PMT) at 800 V. The working electrode was the hybrid-nanomaterial-modified ITO electrode. An Ag/AgCl (saturated KCl) reference electrode was used for all measurements. A platinum wire was used as a counterelectrode.

Preparation of nanoparticles supported on the $[Ru(bpy)_3]^{2+}$-doped silica/Fe_3O_4 nanocomposite: Fe_3O_4 spheres with high saturation magnetization were synthesized by a polyol media solvothermal method according to reference [19] with some modifications. The GNRSF was prepared by the following process: Fe_3O_4 spheres (26 mg) were added to ethanol (30 mL), followed by the addition of TEOS (800 μL), $[Ru(bpy)_3]^{2+}$ (0.1 M, 300 μL), and NH_4OH (25%, 2 mL). The resulting solution was then sonicated for ~6 h and stored overnight. After collection of the precipitate, the resulting product was dissolved in ethanol (20 mL) followed by the addition of H_2O (2 mL), NH_4OH (25%, 2 mL), and APTMS (100 μL). After sonication for 3 h, the NH_2-functionalized hybrid material was collected with an external magnetic field and dissolved in H_2O (20 mL). The gold nano-

particles ($\varnothing \sim 13$ nm) were synthesized according to reference [20]. Finally, the GNRSF was prepared by mixing 3 mL of the above solution with 15 mL of the solution of gold nanoparticles. The resulting product was collected and dissolved in 3 mL H_2O.

Immobilization of the hybrid nanomaterial on the bare ITO electrode surface: A sample (20 μL) of the GNRSF suspension in H_2O was placed on an ITO electrode and air-dried at room temperature. ECL measurements were carried out in PBS (0.1 M, pH 7.5) at a scan rate of $100\ mV\,s^{-1}$. An external magnetic field was placed on the side of beaker for effectively immobilizing hybrid nanomaterials.

[1] J. B. Noffsinger, N. D. Danielson, *J. Chromatogr. A* **1987**, *387*, 520.
[2] A. Arora, J. C. T. Eijkel, W. E. Morf, A. Manz, *Anal. Chem.* **2001**, *73*, 3282.
[3] A. W. Knight, *TrAC Trends Anal. Chem.* **1999**, *18*, 47.
[4] R. C. Engstrom, K. W. Johnson, S. DesJarlais, *Anal. Chem.* **1987**, *59*, 670.

FULL PAPERS

[5] V. G. Kozlov, V. Bulovic, P. E. Burrows, S. R. Forrest, *Nature* **1997**, *389*, 362.

[6] M. M. Richter, *Chem. Rev.* **2004**, *104*, 3003.

[7] C. H. Lyons, E. D. Abbas, J.-K. Lee, M. F. Rubner, *J. Am. Chem. Soc.* **1998**, *120*, 12100.

[8] a) W.-Y. Lee, T. A. Nieman, *Anal. Chem.* **1995**, *67*, 1789; b) H. Y. Wang, G. B. Xu, S. J. Dong, *Electroanalysis* **2002**, *14*, 853; c) A. N. Khramov, M. M. Collinson, *Anal. Chem.* **2000**, *72*, 2943.

[9] H. N. Choi, S.-H. Cho, W.-Y. Lee, *Anal. Chem.* **2003**, *75*, 4250.

[10] a) Z. Guo, S. Dong, *Anal. Chem.* **2004**, *76*, 268; b) J. Li, Y. Xu, H. Wei, T. Huo, E. Wang, *Anal. Chem.* **2007**, *79*, 5439; c) S. Guo, E. Wang, *Electrochem. Commun.* **2007**, *9*, 1252.

[11] a) M. M. Collinson, B. Novak, S. A. Martin, J. S. Taussig, *Anal. Chem.* **2000**, *72*, 2914; b) M. Sykora, T. J. Meyer, *Chem. Mater.* **1999**, *11*, 1186.

[12] a) Y. Du, B. Qi, X. Yang, E. Wang, *J. Phys. Chem. B* **2006**, *110*, 21662; b) X. Sun, Y. Du, L. Zhang, S. Dong, E. Wang, *Anal. Chem.* **2006**, *78*, 6674.

[13] L. Zhang, S. Dong, *Anal. Chem.* **2006**, *78*, 5119.

[14] a) X. Sun, Y. Du, S. Dong, E. Wang, *Anal. Chem.* **2005**, *77*, 8166; b) X. Sun, Y. Du, L. Zhang, S. Dong, E. Wang, *Chem. Asian J.* **2007**, *2*, 1137.

[15] A. Lu, E. L. Salabas, F. Schüth, *Angew. Chem.* **2007**, *119*, 1242; *Angew. Chem. Int. Ed.* **2007**, *46*, 1222.

[16] D. Kim, Y. Lyu, H. N. Choi, I. Min, W. Lee, *Chem. Commun.* **2005**, 2966.

[17] L. Zhang, B. Liu, S. Dong, *J. Phys. Chem. B* **2007**, *111*, 10448.

[18] a) D. Tang, R. Yuan, Y. Chai, H. An, *Adv. Funct. Mater.* **2007**, *17*, 976; b) J. Ge, Y. Hu, T. Zhang, Y. Yin, *J. Am. Chem. Soc.* **2007**, *129*, 8974; c) X. Xu, C. Deng, M. Gao, W. Yu, P. Yang, X. Zhang, *Adv. Mater.* **2006**, *18*, 3289.

[19] H. Deng, X. L. Li, Q. Peng, X. Wang, J. P. Chen, Y. D. Li, *Angew. Chem.* **2005**, *117*, 2842; *Angew. Chem. Int. Ed.* **2005**, *44*, 2782.

[20] Y. Wang, H. Wei, B. Li, W. Ren, S. Guo, S. Dong, E. Wang, *Chem. Commun.* **2007**, 5220.